

# **FRACTURE OF NANOSTRUCTURED FCC METALS**

F. Ebrahimi, Z. Ahmed K. L. Morgan and A. J. Liscano

Materials Science and Engineering, University of Florida  
P.O. Box 116400, Gainesville, FL 32611

## **ABSTRACT**

Nanocrystalline nickel and nanolayered structures of nickel and copper were produced by electrodeposition techniques. The analysis of the fracture surfaces of tensile specimens from these materials revealed that the low tensile elongation of nanostructured metallic materials is associated with a strong tendency to strain localization and the presence of pores in the microstructure.

## **KEYWORDS**

nanostructures, nanocrystalline, multilayers, electrodeposition, nickel, copper, fracture, ductility

## **INTRODUCTION**

The term “nanostructure” has been used to describe: (1) materials with at least one of their physical dimensions in the nano-range (e.g., particles or wires with nano-size diameters) and (ii) bulk materials (physical dimensions much larger than nano-size) whose microstructural constituents are in the nano-range (e.g., nanocrystalline and nanolayered materials). The nano-size is conventionally referred to lengths less than 100nm [1]. Due to the confinement of dislocations, bulk metallic nanostructures have very high yield strengths. However, the tensile testing results indicate that these materials exhibit low total elongations [2]. Processing defects have been suggested to be the cause of the low ductility of nanocrystalline FCC (face-centered cubic) metals produced via the gas condensation method [3]. We have been successful in fabricating almost defect free nanocrystalline and nanolayered metallic structures from FCC metals using electrodeposition techniques [4]. This paper presents results regarding the fracture behavior of nanocrystalline nickel and nanolayered nickel/copper materials and discusses the low elongation of metallic nanostructures.

## **EXPERIMENTAL PROCEDURES**

The details of the fabrication of the nanomaterials using electrodeposition techniques are given elsewhere [4-7]. The deposits were in the form of discs with a 35mm diameter and were grown on copper substrates, which were subsequently dissolved. The deposits had a thickness between 25 to 40 $\mu$ m. Free-standing tensile specimens with a gage length of 10mm were prepared by hand grinding and were tested at a strain rate of  $2 \times 10^{-4} \text{ s}^{-1}$ . At least two tensile specimens were tested per deposit. The fracture surfaces were studied using scanning electron microscopy (SEM).

## RESULTS AND DISCUSSION

### *Nanocrystalline Nickel*

Changing the electrodeposition parameters can vary the grain size of nickel deposits. Table 1 presents the grain size for nickel deposits fabricated at 18 and 25 mA/cm<sup>2</sup> using direct current (DC) and at 25mA/cm<sup>2</sup> by pulse plating. The grain size was measured using x-ray diffraction and applying the Warren-Averbach analysis method. Note that the grain size may vary through the thickness of the deposits. Therefore, the grain size was measured on both the substrate and the solution sides of the deposits. The tensile stress-strain curves for these deposits are presented in Figure 1. The tensile specimens from the same deposit showed similar yield strength and strain hardening rates; however, there was a noticeable scatter in the total elongation.

TABLE 1  
GRAIN SIZE OF THE NANOCRYSTALLINE NICKEL SAMPLES

Deposition Condition	Grain Size (nm)	
	Substrate	Solution
25 mA/cm <sup>2</sup> - pulsed	10	9
25 mA/cm <sup>2</sup> - DC	35	17
18 mA/cm <sup>2</sup> -DC	111	11

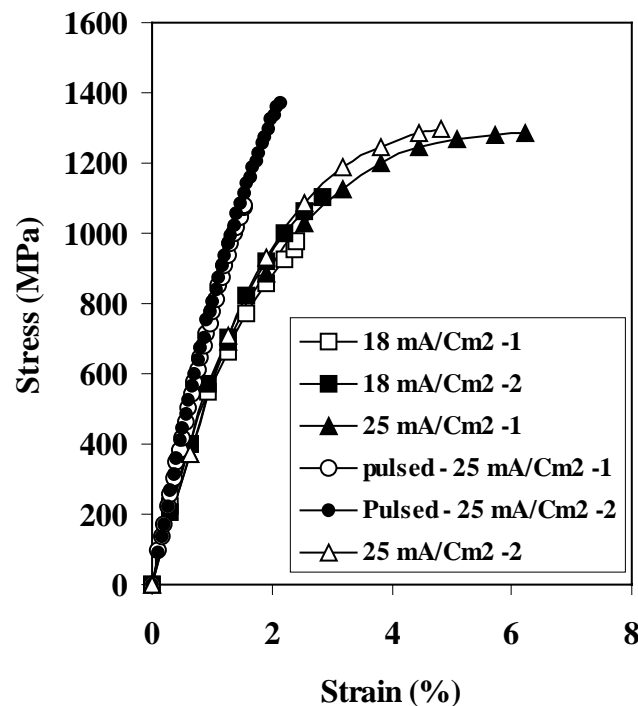


**Figure 1:** Tensile stress strain curves for three nanocrystalline nickel deposits.

Examples of the fracture surface of the nanocrystalline nickel samples are given in Figure 2. All samples necked before fracture, although none of them showed any post-neck elongation according to the stress-strain curves. This observation shows that the necking process was very localized in these materials. Since such a behavior is not observed in thin samples of metals with conventional grain sizes [8], the strong tendency to strain localization is indicative of a low strain-rate sensitivity of nanocrystalline nickel. Hydrogen incorporation during the deposition may also contribute to this effect. However, the grain boundary sliding mechanism, which has been suggested to operate in nanocrystalline materials at a low homologous temperature [9], is not expected to contribute significantly to the deformation of nanocrystalline nickel samples studied here. The two DC-plated deposits showed similar strength levels, but the deposit made at 18 mA/cm<sup>2</sup> showed a lower ductility than the sample deposited at 25 mA/cm<sup>2</sup>. The fractographs presented in Figure 2 show that fracture in the former deposit occurred by microvoid coalescence mechanism while the latter deposit broke by the so-called

knife-edge mechanism, typical of pure defect free metals. During the electrodeposition of nickel hydrogen evolves at the cathode surface and bubbles develop on the deposition front which depending on the cathode surface condition, electrolyte composition and the local hydrodynamic state may get trapped in the deposit. These bubbles act as initiation sites for the microvoids observed on the fracture surface.

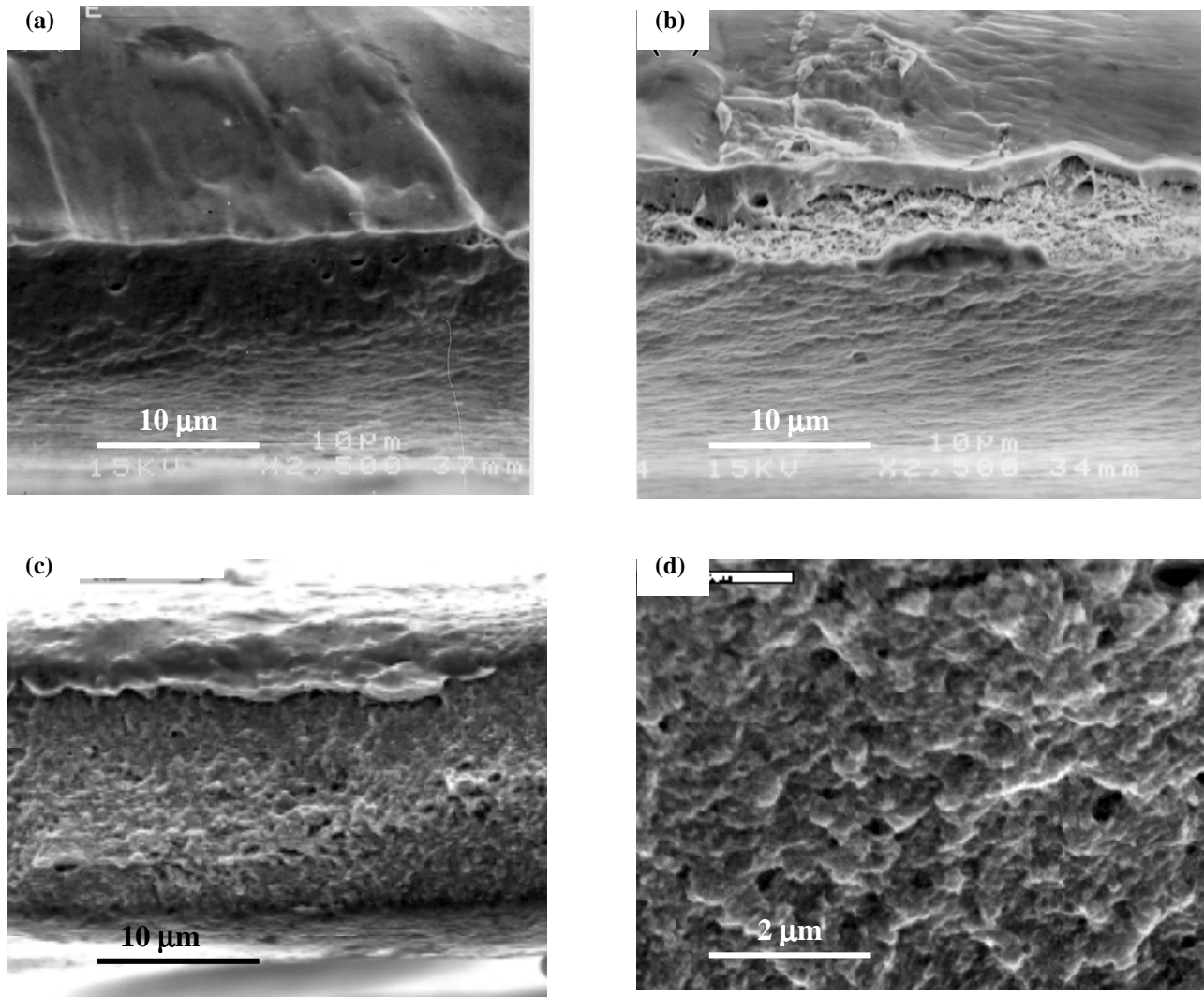


**Figure 2:** Fracture surfaces of tensile samples from deposits produced at (a)  $25 \text{ mA/cm}^2$ , DC-plated, (b)  $18 \text{ mA/cm}^2$ , DC-plated and (c)  $25 \text{ mA/cm}^2$ , pulse plated. A high magnification picture of the fracture surface shown in (c) is presented in (d).

Figure 3 shows the strain-hardening rate as a function of strain for the two DC deposited samples. Note that the Considère necking criterion ( $d\sigma/d\varepsilon$  (strain hardening rate) =  $\sigma_{UTS}$  (ultimate tensile strength)) for the high ductility deposit ( $25 \text{ mA/cm}^2$ ) is approximately satisfied, however, the necking occurred prematurely in the low ductility deposit ( $18 \text{ mA/cm}^2$ ). It is suggested that the pores formed due to the entrapment of the hydrogen bubbles promoted plastic instability.

The deposit produced using the pulse-plating method showed the smallest grain size, the highest yield strength and the lowest ductility. The tensile specimens from this deposit exhibited limited necking (Figure 2c) and the fracture surface resembled the quasi-cleavage fracture behavior usually observed in materials such as high carbon steels (Figure 2d).

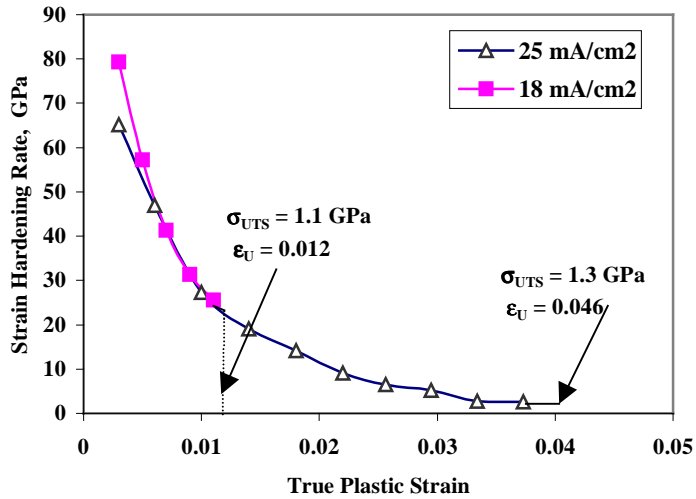


**Figure 3:** Strain-hardening rate as a function of true plastic strain showing that necking occurred at  $d\sigma/d\varepsilon \gg \sigma_{UTS}$  in the sample fabricated at  $18 \text{ mA/cm}^2$ .

### *Nanolayered Nickel-Copper Structures*

The nanolayered Ni/Cu materials showed a variety of fracture behaviors depending on the microstructure and the level of defects of the deposits. Figure 4 shows the stress-strain curve and the fracture surface of a defect-free multilayered Ni/Cu sample with a bi-layer thickness of 7nm. This sample exhibited a low total elongation but it was very ductile as indicated by the knife-edge fracture behavior. It should be noted that at the bi-layer thickness of 7nm, the interface between nickel and copper is most probably coherent and dislocations are not confined by the presence of the interfaces. The low total elongation of this sample indicates that shear localization occurs easily in these metallic nanostructures.

In deposits that hydrogen bubble entrapment was a problem, fracture of the Ni/Cu multilayered structures occurred by microvoid coalescence mechanism. The observation of the microvoid coalescence mechanism was dependent on the stress-state. The plane-stress condition near the edges of the samples decreased the possibility of microvoid growth and resulted in the knife-edge fracture behavior.

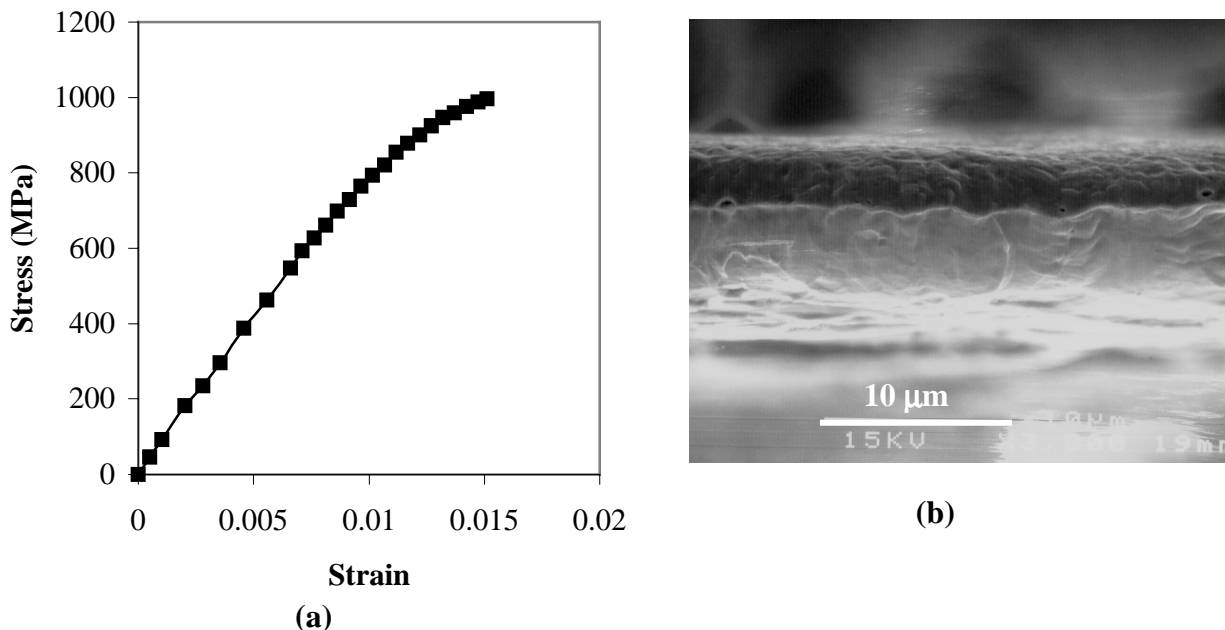


**Figure 4:** (a) Tensile stress-strain curve and (b) SEM fractograph of a multilayered Ni/Cu sample showing a low total elongation associated with a ductile fracture behavior.

The fractographs from a relatively brittle multilayered Ni/Cu sample with a bi-layer thickness of 20nm is presented in Figure 5. This sample broke in the linear portion of the stress-strain curve. Several fracture paths can be noticed in these fractographs. The gaps due to the incomplete growth of columns have led to the intercolumnar fracture path. The delamination of the layers is observable near the substrate side of this deposit. The high magnification picture presented in Figures 5b shows the quasi-cleavage facets similar to those observed in the nanocrystalline nickel deposit with the lowest ductility (see Figure 2d).

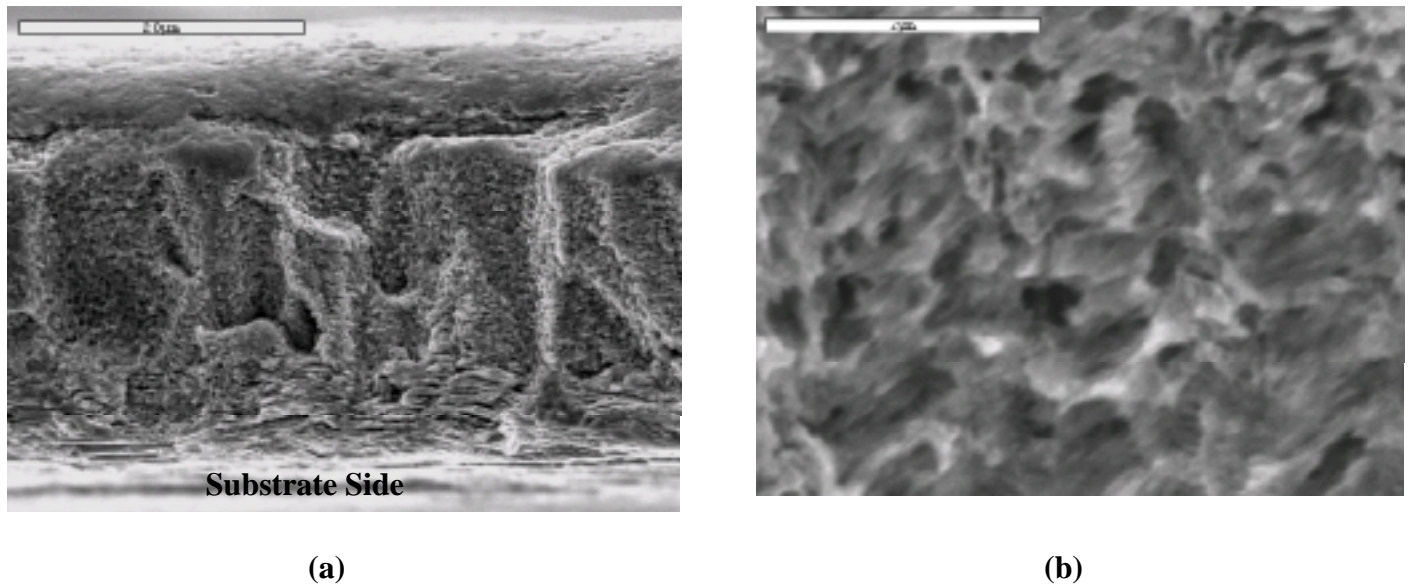


**Figure 5:** (a) SEM micrograph showing the intercolumnar and the interlayer fracture behaviors in a Ni/Cu nanolayered structure. (b) A high magnification fractograph showing large voids and quasi-cleavage facets.

### ***Brittle Fracture in FCC Metals***

Usually, FCC metals do not fracture in a brittle manner. There are two possible mechanisms that can explain the development of quasi-cleavage facets in the FCC metallic nanostructures studied here. One scenario is that the ligaments between the pores, which form by the entrapment of hydrogen bubbles, tear in mode III. Such a process can be envisioned to occur by the generation and motion of screw dislocations from the pore surfaces. Theoretically it has been shown that spontaneous dislocation generation from the crack tip makes the breaking of atomic bonds in FCC metals such as Ni and Cu impossible [10]. However, such models do not take into account the limitation on the size of the dislocation loops that can emerge from the crack tip because of the presence of interfaces and boundaries. Therefore, the other possibility is that due to the confinement of dislocations in metallic nanostructures, the local stresses near the processing defects such as pores can be raised high enough to break the atomic bonds in mode I. We have shown that the quasi cleavage fracture develops in the mid-section of tensile samples under the plane-strain condition and the fracture behavior changes to the microvoid coalescence mechanism under the plane stress condition that develops near the edges [11,12]. These observations suggest that the brittle fracture in FCC metallic nanostructures may occur by the cleavage mechanism, i.e. breaking atomic bonds under mode I loading.

## **CONCLUSIONS**

Nanocrystalline nickel and nanolayered nickel/copper structures were fabricated by electrodeposition techniques. Their strength, ductility and fracture behaviors were investigated by tensile testing of dog-bone samples. The results of this study show that the low total elongation of these nanostructures in the absence of any processing defects is associated with a strong tendency to strain localization. It has been suggested that hydrogen gas bubbles form on the cathode surface during deposition. These bubbles become entrapped as pores into the deposits. These pores act as initiation sites for fracture by the microvoid coalescence mechanism. In structures that dislocation generation/motion is inhibited (e.g., nanocrystals with small grain size and nanolayered

structures with incoherent boundaries), fracture in between the pores occurs by breaking atomic bonds, i.e. cleavage mechanism.

## ACKNOWLEDGEMENTS

The authors gratefully acknowledge the financial support of National Science Foundation under the contract number DMR – 9980213.

## REFERENCES

1. H. Gleiter, *Materials Science Forum* 189-190, 67 (1995).
2. C. C. Koch, D. G. Morris, K. Lu, and A. Inoue, *MRS Bulletin* 24, 54 (1999).
3. P. G. Sanders, C. J. Youngdahl, J. R. Weertman, *Mater. Sci. Eng.* A234-236, 77 (1997).
4. F. Ebrahimi, D. Kong, T. E. Matthews, and Q. Zhai, in Processing and Fabrication of Advanced Materials VII, TMS Publication, Warrendale, PA, 509 (1998).
5. F. Ebrahimi, G. R. Bourne, M. S. Kelly, and T. E. Matthews, *Nanostructured Materials Journal* 11(3), 343 (1999).
6. F. Ebrahimi and D. Kong, *Scripta Materialia*, 40, 609 (1999).
7. F. Ebrahimi and A. J. Liscano, *Mater. Sci. Eng.* A301, 23 (2001).
8. F. Ebrahimi, Q. Zhai and D. Kong, *Scripta matter.* 39, 315 (1998).
9. R. M. Masumura, P. M. Hazzeldine, and C. S. Pande, *Acta matter.* 46, 4527 (1998).
10. J. R. Rice and R. Thomson: *Phil. Mag.* 29, 73 (1974).
11. F. Ebrahimi, Q. Zhai, and D. Kong, *Materials Science and Engineering*, 255, 20 (1998).
12. F. Ebrahimi, Q. Zhai, D. Kong, and G. R. Bourne, in Advanced Materials for 21<sup>st</sup> Century: The 1999 Julia Weertman Symposium, Edited by Y-W. Chung et al., TMS Publication, Warrendale Pacific, 421 (1999).